Weak ferromagnetism in CoF_2 and NiF_2

A. N. Bazhan and Ch. Bazan[1)]

Institute of Physics Problems, USSR Academy of Sciences
(Submitted June 16, 1975)
Zh. Eksp. Teor. Fiz. **69**, 1768–1781 (November 1975)

The anisotropy of the magnetic properties of CoF_2 and NiF_2 single crystals is investigated with an oscillating-sample magnetometer. The magnetic moment can be measured along three mutually perpendicular directions at $T = 4.2$ K and at field strengths between 0 and 140 kOe. It has previously been shown [A.S. Borovik-Romanov, 1962; V. I. Ozhogin, 1965] for CoF_2 that in the absence of a magnetic field the antiferromagnetic vector **L** is parallel to the tetragonal axis [001]. If the magnetic field **H** ∥ [100], the antiferromagnetic vector **L** rotates in the plane (001) with increasing **H** and a state with transverse weak ferromagnetism $\sigma_{D\perp}$ arises. The rotation of *L* occurs in a plane perpendicular to **H**. It is demonstrated in the present paper that if **H** ∥ [110], the rotation of **L** in weak fields occurs in the $(1\bar{1}0)$ plane and in this case a state arises which possesses weak ferromagnetism $\sigma_{D\parallel}$ along the antiferromagnetic vector **L** and transverse weak ferromagnetism $\sigma_{D\perp} \perp$ **L**. With increase of the magnetic field strength **H**, the vector **L** turns in a direction perpendicular to **H**, i.e., to the [010] axis. The NiF_2 measurements are a continuation of our previous work [with A. S. Borovik-Romanov and N. M. Kreines, 1973] in the high field range. They confirm that if **H** ∥ [110], then on increase of magnetic field strength the antiferromagnetic vector turns away from the [100] axis to [110]. In this case a state with longitudinal weak ferromagnetism $\sigma_{D\parallel}$ arises. In fields of the order of 140 kOe the rotation angle is of the order of 30°. The values of $\sigma_{D\perp}$ and $\sigma_{D\parallel}$ for CoF_2 and NiF_2 are determined.

PACS numbers: 75.50.Dd

The theory developed by Dzyaloshinskiĭ [1] for weak ferromagnetism in antiferromagnets deals with two models of the onset of the weak ferromagnetism. In the first model the weak ferromagnetism results from the shear of the magnetization vectors of the sublattices of the antiferromagnets—transverse weak ferromagnetism $\sigma D\perp$, and in the second model the weak ferromagnetism is the consequence of the inequality of the magnetizations of the sublattices when they are strictly antiparallel—"longitudinal" weak ferromagnetism $\sigma D\parallel$. In all the antiferromagnets studied to date (rhombohedral) structures, orthoferrites, and others), the transverse weak ferromagnetism $\sigma D\perp$ was observed. From among the known antiferromagnets, longitudinal weak ferromagnetism is possible in the nickel and cobalt fluorides NiF_2 and CoF_2.

These fluorides have tetragonal symmetry[1] D_{4h}^{14}. In the antiferromagnetic state of CoF_2 ($T_N = 37.7°K$)[2-4] in the absence of a magnetic field, the antiferromagnetic vector **L** is directed along the tetragonal axis [001], and there is no weak ferromagnetism. In investigations of the piezomagnetic effect, Borovik-Romanov[5] was the first to show that in CoF_2 there is produced, besides the piezomagnetic moment perpendicular to the magnetization direction of the sublattice and equivalent to the transverse weak ferromagnetism $\sigma D\perp$, also a magnetic moment parallel to the sublattice magnetization and equivalent to the longitudinal weak ferromagnetism $\sigma D\parallel$.

In NiF^2 ($T_N = 73.2°K$)[6-9] the antiferromagnetic vector **L** lies in a plane perpendicular to the tetragonal axis, along the twofold axis [100] or [010]; NiF_2 is then a weak ferromagnet. Investigation of the weak ferromagnetism of NiF_2 has shown that in weak magnetic fields and in strong fields **H** ∥ [010] the antiferromagnetic vector **L** ∥ [100] and the spontaneous magnetic moment $\sigma_{D\perp}$ is the result of the shear of the magnetic moments of the sublattices.[8,9] Borovik-Romanov, Kreĭnes, and the author[7-8] have established that if **H** ∥ [110], then the antiferromagnetic vector **L** rotates with increasing H from the [100] axis towards the $[1\bar{1}0]$ axis, which is perpendicular to **H**; the transverse weak ferromagnetism $\sigma D\perp$ then vanishes and a longitudinal weak ferromagnetism $\sigma D\parallel$ appears and is parallel to the antiferromagnetic vector **L**. The values of the transverse weak ferromagnetism $\sigma D\perp$, of the transverse magnetic susceptibility $\chi\perp$, of the longitudinal weak ferromagnetism $\sigma D\parallel$ and of the longitudinal magnetic susceptibility $\chi\parallel$ for NiF_2, which were obtained earlier[7,10], are listed in the table. The author has previously[10] proposed a theoretical model for the calculations of the antiferromagnetic resonance (AFMR) frequencies at **H** ∥ [010] for NiF_2 with $\sigma D\parallel$ and $\chi\parallel$ taken into account.

In the case of cobalt fluoride CoF_2, Ozhogin[11] has shown that if a magnetic field **H** is applied to the tetragonal axis [001], then the antiferromagnetic vector **L** is rotated from a state **L** ∥ [001] to a state **L** ⊥ [001]. Further, if **H** ∥ [100], a state is produced with weak transverse ferromagnetism $\sigma D\perp$ and with a magnetic susceptibility $\chi\parallel$ (the values of $\sigma D\perp$ and $\chi\parallel$ are given in the table). On the other hand if **H** ∥ [110], then a state with weak ferromagnetism σD is also produced, but the values of the ferromagnetic moment σD and of the magnetic susceptibility differ from the values $\sigma D\perp$ and $\chi\perp$ at **H** ∥ [100]. Ozhogin[11] and Foner[12] have determined, from experiments made at **H** ∥ [001] (**H** ∥ **L**), the value of the longitudinal magnetic susceptibility $\chi\parallel = (1.1 \pm 0.2) \times 10^{-3}$ cgs emu/mole, while Gufan et al.[13], by investigating AFMR in CoF_2 at **H** ∥ [010] and by means of a theoretical analysis, have demonstrated the possibility of taking into account the effective field responsible for $\sigma D\parallel$ in the expression for the AFMR frequencies.

The purpose of this work was a continuation of the investigation of the magnetic properties of NiF_2 in strong magnetic fields H up to 140 kOe (a magnetic field H up to 65 kOe was used in the previous work[7,10]), to study the anisotropy of the magnetic properties of CoF_2, and to assess the possibility of the existence of longitudinal weak ferromagnetism $\sigma D\parallel$ in CoF_2.

The experiments were performed with the vibrating-sample magnetometer[14] of our Institute which made it

possible to measure the magnetic moment of the sample along three mutually perpendicular directions at H < 65 kOe, and with the vibrating-sample magnetometer of the International Laboratory of Low Temperatures and Magnetic Fields (Wroclaw, Poland) at H < 140 kOe, in which (Fig. 1) we also used a procedure of measuring the magnetic moments both parallel to the applied magnetic field ($M_{\parallel}(H)$ (coils L_1, Fig. 1), and perpendicular to it, $M_{\perp}(H)$ (coils L_2, Fig. 1). The measurements were made on CoF_2 single crystals (m ~ 20 mg) and of NiF_2 (m ~ 5 mg), grown by S. V. Petrov at our Institute.[2)] The accuracy with which the magnetic field H was oriented relative to the crystal axes in the experiments was 2–3°.

MEASUREMENT RESULTS

Figure 2a shows plots of the magnetic moment $M_{\parallel}$ along the magnetic field for CoF_2 against the applied magnetic field H in cases when the field is parallel to the tetragonal axis [001], H ∥ [001], and to the binary axes [010] and [110]. The figure shows also Ozhogin's experimental data.

If the magnetic field H is directed along the tetragonal axis [001] (H < 65 kOe, curve 1 of Fig. 2a), then the plot of the magnetic moment $M_{\parallel}(H)$ takes the form $M_{\parallel}(H) = \chi_{\parallel}H$, where $\chi_{\parallel}$ (see the table) agrees within 5% with the value obtained by Ozhogin[11] and Foner[12].

If the magnetic field is applied along the binary axis [010] (curve 2), then at low values of the magnetic fields, H < 40 kOe, a linear relation $M_{\parallel}(H) = \chi_{\perp}^{*}H$ is observed; with increasing magnetic field, 40 < H < 126 kOe, the $M_{\parallel}(H)$ plot becomes nonlinear, and at H > 126 kOe, according to Ozhogin,[11] it is described by the expression $M_{\parallel}(H) = \sigma D_{\perp} + \chi_{\perp}H$. The values of $\chi_{\perp}^{*}$, $\sigma_{D\perp}$, and $\chi_{\perp}$ obtained in the present study and by Ozhogin[11] and Foner[12] are listed in the table.

If the magnetic field is applied along the binary axis [110] (curve 3), then in weak fields H < 40 kOe the magnetic moment is likewise linear in the field, $M_{\parallel}(H) = \chi_{\perp}^{**}H$, where $\chi_{\perp}^{**} = (6.2 \pm 0.2) \times 10^{-3}$ cgs emu/mole coincides within experimental accuracy with the value $\chi_{\perp}^{*}$ in the case of magnetic field applied along the binary axis [010].

When the orientation of the applied magnetic field is varied in a plane perpendicular to the tetragonal axis [001], the dependence of the magnetic moment along the magnetic field, $M_{\parallel}(H) = \chi_{\parallel}^{*}H$, in weak fields H < 40 kOe remains practically unchanged. When the magnetic field changes from 40 to 120 kOe, as seen from Fig. 2, a nonlinear $M_{\parallel}(H)$ dependence is observed, and at H > 120 kOe this dependence is described, at the accuracy of our experiment and when Ozhogin's data[11] are used, by the expression $M_{\parallel}(H) = \sigma_D^{*} + \chi^{*}H$, where $\sigma_D^{*} = 3000 \pm 200$ cgs emu/mole and $\chi^{*} = (2.3 \pm 0.2) \times 10^{-3}$ cgs emu/mole.

Figure 2b shows plots of $M_{\perp}(H)$ in the (001) plane at H ∥ [010] and at H ∥ [110] (to remagnetize the sample into a one-domain state, the magnetic field H was inclined 5° to the [110] axis). As seen from Fig. 2b, at H ∥ [010] the magnetic moment is $M_{\perp} = 0$ for all values of the magnetic field. At H ∥ [110] and H > 80 kOe, a moment $M_{\perp}(H)$ appears with increasing magnetic field and varies linearly with the applied magnetic field.

Figure 3 shows plots of the magnetic moment $M_{\perp}(H)$ in the (001) plane, perpendicular to the applied magnetic field[14], at H < 65 kOe and at different orientations of the applied magnetic field in this plane. It is seen from Fig. 3 that with increasing H there appears a magnetic moment $M_{\perp}(H)$ that depends nonlinearly on H. At $\psi = 0$ (H ∥ [100]) this moment is small. $M_{\perp}(H)$ increases with increasing angle ψ and reaches a maximum at $\psi = 22$–$23°$. With further increase of ψ, the value of $M_{\perp}(H)$ decreases, and at $\psi = 45°$ (H ∥ [110]), it again becomes small. At $\psi > 45°$ the sign of $M_{\perp}(H)$ is reversed and on the whole all the curves for the corresponding angles $90° - \psi$ are duplicates, with the sign reversed, of the curves for the angles ψ.

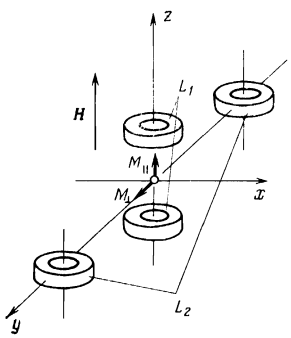

FIG. 1. Arrangement of the measuring coils L_1 (to measure $M_{\parallel}(H)$ and L_2 (to measure $M_{\perp}(H)$) relative to the applied magnetic field H.

Material	$\chi_{\perp}^{*} \cdot 10^3$	$\chi_{\perp} \cdot 10^3$	$\sigma_{D\perp}$	$\chi_{\parallel} \cdot 10^3$	$\sigma_{D\parallel}$	Source
CoF_2	6.4±0.2	2.3±0.2	5300±200	1.0±0.2	–	[11]
	6.2±0.1	–	–	1.1±0.1	–	[12]
	6.3±0.2	2.6±0.3	5200±200	1.1±0.2	3700±400	Present work
NiF_2		6.55±0.3	172±5	–	–	[8]
		6.02±0.05	161.5±0.3	–	69±4	[9]
		6.2±0.1	169±0.2	1.2±0.2	73±4	[7, 10]
		6.2±0.1	169±2	1.2±0.2	71±10	Present work

*The values of χ and σ are in cgs emu/mole.

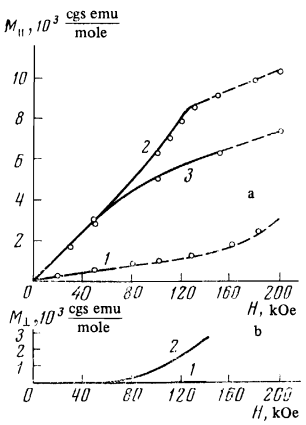

FIG. 2. a) Plot of $M_{\parallel}(H)$ for CoF_2 at H ∥ [001] – curve 1, H ∥ [010] – curve 2, and H ∥ [110] – curve 3. Solid curves – present results, ○ – results of [11]. b) Plots of $M_{\perp}(H)$ at H ∥ [010] – curve 1 and H ∥ [110] – curve 2.

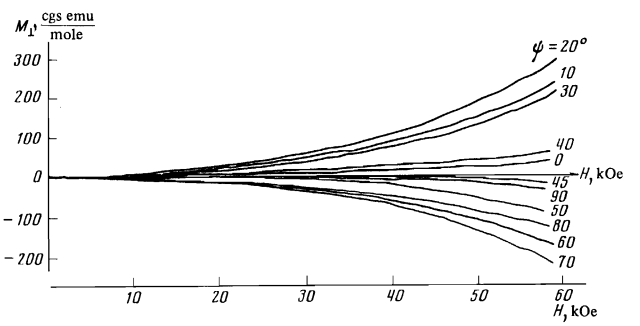

FIG. 3. Dependence of the magnetic moment $M_{\perp}(H)$ for CoF_2 with changing orientation of the applied magnetic field in the (001) plane.

Figure 4 shows plots of $M_\perp^z(H)$, the magnetic moment perpendicular to the applied magnetic field, measured along the tetragonal axis [001] for different orientations of **H** in the (001) plane. It is seen from Fig. 4 that if **H** ∥ [110] ($\psi = 45°$), then $M_\perp^z$ depends nonlinearly on the applied magnetic field **H**, but if **H** ∥ [010], then the observed value of $M_\perp^z$ is small.

Figure 5 shows plots of $M_\perp^z(\psi)$ with changing orientation of **H** in the (001) plane. It is seen from Fig. 5a that at H = 10 kOe we have $M_\perp^z(\psi) = A \sin \psi$; this appears to be the consequence of the onset of a small magnetic moment $M_\perp^z(H)$ due to the inexact orientation of the applied magnetic field relative to the crystal axes. At H = 50 kOe, a more complicated $M_\perp^z(\psi)$ dependence is observed. It is seen from Fig. 5b that at **H** ∥ [110] maxima of $M_\perp^z(\psi)$ appear. This form of $M_\perp^z(\psi)$ is described by the expression

$$M_\perp^z(\psi) = B \sin 2\psi \operatorname{sgn} \sin \psi + C \sin \psi.$$

The dashed line in Fig. 5b denotes the function $M_\perp^z(H) = B \sin 2\psi \operatorname{sign} \sin \psi$. It is seen from Fig. 5b that at

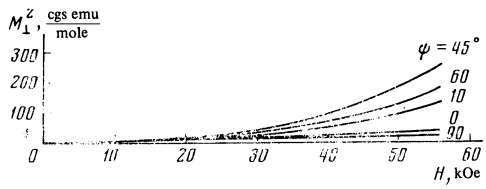

FIG. 4. Dependence of the magnetic moment $M_\perp^z(H)$ for CoF_2 with changing orientation of the applied magnetic field in the (001) plane.

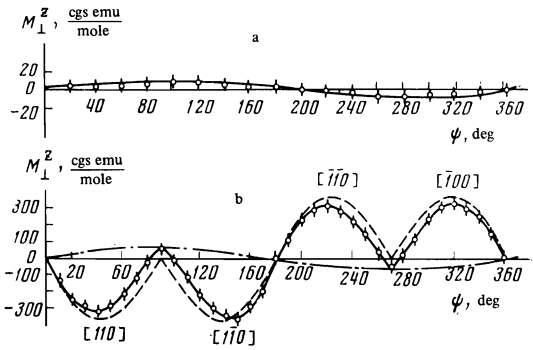

FIG. 5. Dependence of the magnetic moment $M_\perp^z$ of CoF_2 on the orientation of **H** in the (001) plane: a—plot of $M_\perp^z(\psi)$ at H = 10 kOe, b—at H = 50 kOe.

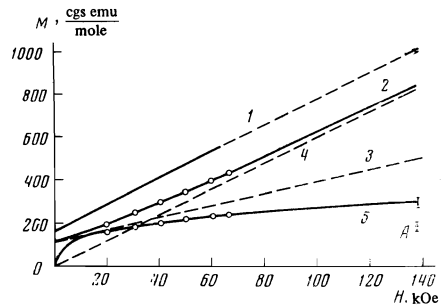

FIG. 6. Dependence of the magnetic moment $M_\parallel(H)$ of NiF_2 at **H** ∥ [010] (curve 1) and **H** ∥ [110] (curve 2); plots of $M_\parallel(H) = 2^{-1/2}\sigma D_\perp + 1/2\chi H$ (curve 3) and $M_\parallel(H) = \chi_1(H)$ (curve 4); plot of the magnetic moment $M_\perp(H)$ at **H** ∥ [110] (curve 5). Solid curve—present results, ○—data of [7]. The vertical bar on curve 5 indicates the experimental error with allowance for the produced parasitic signals induced in the measuring coils L_1 and L_2 (Fig. 1) when the magnetic field H is increased.

H = 50 kOe and **H** ∥ [110] we have $M_\perp^{z0}$ = B = 360 ± 30 cgs emu/mole.

Figure 6 shows plots of $M_\parallel(H)$ for NiF_2 at **H** ∥ [010] and **H** ∥ [110]. The same figure shows the data from from[7,10]. It is seen from the figure that, just as before[7,10], a nonlinear $M_\parallel(H)$ dependence is observed at **H** ∥ [110].

With increasing magnetic field, the experimental $M_\parallel(H)$ dependence (Fig. 6, curve 2), deviates from the dependence described by the expression $M_\parallel(H) = 2^{-1/2}\sigma D_\perp + 1/2\chi_\perp H$ (curve 3) obtained at **H** ∥ [110] under the assumption that the antiferromagnetic vector **L** is directed exactly along the [110] axis, and approaches asymptotically the linear relation described by the expression $M_\parallel(H) = \chi_\perp H$ (curve 4) obtained at **H** ∥ [110] under the assumption that the antiferromagnetic vector **L** ⊥ **H**. The values of $\sigma_{D\perp}$ and $\chi_\perp$ are listed in the table.

Curve 5 of Fig. 6 shows a plot of $M_\perp(H)$ in the (001) plane at **H** ∥ [110] (in the experiment, the magnetic field **H** was directed at an angle ~5° to the [110] axis[7]). It is seen from the figure that $M_\perp(H)$ at **H** ∥ [110] depends nonlinearly on the applied magnetic field. With increasing H, the $M_\perp(H)$ dependence deviates from that described by the expression[7] $M_\perp(H) = 2^{-1/2}\sigma D_\perp + 1/2\chi_\perp H$ in weak fields (Fig. 6, curve 3). In strong magnetic fields, $M_\perp(H)$ depends weakly on the applied magnetic field.

DISCUSSION OF RESULTS

To discuss the experimental results and to compare them with the theory it is necessary to consider, as was done in[1,7,10], the form of the thermodynamic potential of the tetragonal crystal, with account taken of the appearance, in the cobalt and nickel fluorides, of invariants that are responsible for the transverse magnetic susceptibility $\chi_\perp$, the transverse weak ferromagnetism $\sigma D_\perp$, the longitudinal magnetic susceptibility $\chi_\parallel$, and the longitudinal weak ferromagnetism $\sigma D_\parallel$. As shown by Dzyaloshinskiĭ,[1] Such a thermodynamic potential is of the form

$$\Phi = 1/2 a\gamma_z^2 + 1/2 B\mathbf{m}^2 - e(\gamma_x m_y + \gamma_y m_x) + 1/2 D(\gamma\mathbf{m})^2 - 2d(\gamma\mathbf{m})\gamma_x\gamma_y + 1/4 g\gamma_x^2\gamma_y^2 - \mathbf{mH}. \quad (1)$$

Here

$$\sigma_{D\perp} = \frac{e}{B}, \quad \chi_\perp = \frac{1}{B}, \quad \sigma_{D\parallel} = \frac{e+d}{B+D}, \quad \chi_\parallel = \frac{1}{B+D}. \quad (2)$$

Under the condition that $\chi_\parallel \neq 0$, a longitudinal weak ferromagnetism $\sigma D_\parallel$ can appear in CoF_2.[1,7,10] The antiferromagnetic vector $\boldsymbol{\gamma} = \mathbf{L}/|\mathbf{L}|$ then becomes nonorthogonal to the magnetization vector **m**:

$$\gamma\mathbf{m} = 2\frac{e+d}{B+D}\gamma_x\gamma_y + \frac{\mathbf{H}\gamma}{B+D}. \quad (3)$$

Let us examine the experimental results obtained for CoF_2. In accord with the earlier studies,[4,5,11] it follows from the experimental results of Figs. 2 and 3 that if the magnetic field **H** is applied along the [010] axis, then **L** is rotated in a plane perpendicular to the tetragonal axis, and a state with a transverse ferromagnetism is produced. **L** rotates is in a plane perpendicular to **H**, i.e., in the (010) plane. Minimization of the thermodynamic potential (1) with respect to **m** and the angle θ between the direction of the antiferromagnetic vector **L** and the tetragonal axis [001] leads at **H** = [010] to the expressions[11,15]

$$M_{\parallel}(H)=\sigma_{D\perp}\sin\theta+\chi_{\perp}H,\quad M_{\perp}(H)=0,\quad M_{\perp}^{z}(H)=0 \tag{4}$$

and to an equation for the angle of rotation of the antiferromagnetic vector as a function of the applied magnetic field $H < H_c = 125$ kOe:

$$[(H_{AE}^2-H_{D\perp}^2)\sin\theta-H_{D\perp}H]\cos\theta=0. \tag{5}$$

Since $\mathbf{L} \parallel [001]$ at $H = 0$, the constant a in the expression (1) for the thermodynamic potential is negative, and $H_{AE}^2 = -aB$, $H_{D\perp} = e$. We then obtain from (4) and (5) that at $0 < \theta < \pi/2$

$$\sin\theta=\frac{H_{D\perp}H}{H_{AE}^2-H_{D\perp}^2},\quad M_{\parallel}(H)=\sigma_{D\perp}\frac{H}{H_c^*}+\chi_{\perp}H \tag{6}$$

and at $\theta = \pi/2$

$$\sin\theta=1,\quad M_{\parallel}(H)=\sigma_{D\perp}+\chi_{\perp}H,$$

where $H_c^* = (H_{AE}^2 - H_{D\perp}^2)/H_{D\perp}$ is the magnetic field at which the antiferromagnetic vector $\mathbf{L}$ should lie in the (001) plane with allowance for the nonlinearity of $M_{\parallel}(H)$ at $H \sim H_c$.

From a comparison of (6) with the experimental plot of $M_{\parallel}(H)$ (curve 2 of Fig. 2) we see that the function $M_{\parallel}(H) = \chi_{\perp}^* H$ is linear in the applied magnetic field up to 40 kOe, and $\chi_{\perp}^*$ exceeds $\chi_{\perp}$ because of the rotation of the antiferromagnetic vector and because of ensuing transverse weak ferromagnetism $\sigma_{D\perp}$.[11,15]

From the value of $\chi_{\perp}^*$ and from the $\sigma_{D\perp}$ obtained from strong-field data we calculated the value $H_c^* = 150$ kOe. The onset of a nonlinear $M_{\parallel}(H)$ dependence with increasing magnetic field above 40 kOe is attributed[16] to the presence in the thermodynamic potential (1) of CoF_2 of a term $(1/4)f\gamma_z^4$, which increases the rotation of the antiferromagnetic vector $\mathbf{L}$ when H comes closer to H_c, and causes the vector $\mathbf{L}$ to fall in the (001) plane at a field $H_c = 125$ kOe which is smaller than H_c^*. At $H > H_c = 125$ kOe, the moment is $M_{\parallel}(H) = \sigma_{D\perp} + \chi_{\perp}H$ (see formula (6)). The obtained values of $\sigma_{D\perp}$ and $\chi_{\perp}$ correspond on the effective Dzyaloshinskiĭ field $H_{D\perp} = 200 \pm 20$ kOe and to an effective exchange field $H_E = 800 \pm 50$ kOe.

At $\mathbf{H} \parallel [110]$ there is also a rotation of the antiferromagnetic vector $\mathbf{L}$ in a plane perpendicular to the tetragonal axis [001], and this also gives rise to a state with weak ferromagnetism. This is evidenced by the fact that $\chi_{\perp}^{**} > \chi_{\perp}$. To determine the plane in which the rotation of the antiferromagnetic vector L begins in weak fields, it is necessary to compare the obtained experimental values of $M_{\parallel}(H)$ and $M_{\perp}(H)$ (Figs. 2 and 3) at $H \parallel [010]$ and $H \parallel [110]$ with the results of the theoretical calculation of these relations obtained by minimization of the thermodynamic potential (1).

Minimization of the thermodynamic potential (1) with respect to m and the angles θ between the direction of $\mathbf{L}$ and the [001] axis and φ between the direction of $\mathbf{L}$ and the [100] axis in the (001) plane for the case $\mathbf{H} \parallel [110]$ leads to equations for the rotation angles $\varphi(H)$ and $\theta(H)$ of the antiferromagnetic vector $\mathbf{L}$ which are difficult to solve at all values of the magnetic field H, and to complicated relations for the magnetic moments $M_{\parallel}(H)$, $M_{\perp}(H)$, and $M_{\perp}^{z}(H)$. It is possible, however, to carry out the analysis for the case of weak fields $H^2 \ll H_c H_D$ at small values of the rotation angle θ of the antiferromagnetic vector from the tetragonal axis [001] and to compare the results with the experimental data for $M_{\parallel}(H)$ at $\mathbf{H} \parallel [010]$ and $\mathbf{H} \parallel [110]$—Fig. 2—and for $M_{\perp}(H)$ when the orientation of the magnetic field $\mathbf{H}$ is varied in the (001) plane—Fig. 3. It will be shown below that the conclusions of such an analysis are valid up to fields of the order of 40—50 kOe.

Neglecting the $\sin\theta$ terms of order higher than the first in the expressions obtained by minimizing (1) for $\varphi(H)$ and $\theta(H)$, we can obtain these equations in the form

$$\begin{aligned}&(H_{AE}^2-H_{D\perp}^2)\sin\theta-2^{-1/2}H_{D\perp}H(\sin\varphi+\cos\varphi)\\&+{}^1/_2(1-\chi_{\parallel}/\chi_{\perp})H^2(\sin\varphi+\cos\varphi)^2\sin\theta=0,\\&(\cos\varphi-\sin\varphi)\sin\theta[-2^{-1/2}H_{D\perp}H\\&+{}^1/_2(1-\chi_{\parallel}/\chi_{\perp})H^2\sin\theta(\sin\varphi+\cos\varphi)]=0.\end{aligned} \tag{7}$$

In these expressions and below, we use the notation

$$\begin{aligned}&H_{D\perp}=\sigma_{D\perp}/\chi_{\perp}=e,\quad H_{D\parallel}=\sigma_{D\parallel}/\chi_{\parallel}=e+d,\\&H_{AE}^2=aB,\quad H_{AE}^{*2}=gB,\\&H_{D\parallel}^*=\sigma_{D\parallel}/\chi_{\perp}=(e+d)B/(B+D).\end{aligned}$$

Obtaining from the first equation of (7) an expression for $\sin\theta$ and substituting it in the second, we obtain an equation for the angle $\varphi(H)$ in the form

$$\begin{aligned}&(\sin\varphi-\cos\varphi)\sin\theta[-(H_{AE}^2-H_{D\perp}^2)][(H_{AE}^2-H_{D\perp}^2)\\&+{}^1/_2(1-\chi_{\parallel}/\chi_{\perp})H^2(\sin\varphi+\cos\varphi)^2]^{-1}=0.\end{aligned}$$

From this equation it is seen that the rotation of $\mathbf{L}$ should occur in the $(1\bar{1}0)$ plane:

$$\cos\varphi-\sin\varphi=0,\quad \varphi=\pi/4.$$

The expression for $M_{\parallel}(H)$ then takes the form

$$\begin{aligned}M_{\parallel}(H)=&\sigma_{D\perp}\sin\theta-(\sigma_{D\perp}-\sigma_{D\parallel})\sin^3\theta\\&-\chi_{\perp}(1-\chi_{\parallel}/\chi_{\perp})H\sin^2\theta+\chi_{\perp}H.\end{aligned} \tag{8}$$

In (8) and in (7) we can neglect in our case the terms of order higher than the first in H and in $\sin\theta$, and it turns out then that the relation

$$M_{\parallel}(H)=\sigma_{D\perp}\sin\theta+\chi_{\perp}H$$

and the equation for the rotation of $\mathbf{L}$ at $\mathbf{H} \parallel [110]$

$$(H_{AE}^2-H_{D\perp}^2)\sin\theta-H_{D\perp}H=0$$

coincide with the $M_{\parallel}(H)$ dependence and with the rotation equation for the case $\mathbf{H} \parallel [010]$ (see expressions (4) and (5)), in agreement with the experimental data for $M_{\parallel}(H)$ on Fig. 2. It can thus be assumed that in weak magnetic fields at $\mathbf{H} \parallel [110]$ the antiferromagnetic vector $\mathbf{L}$ begins to rotate in the plane $(1\bar{1}0)$.

Another confirmation of the conclusion drawn concerning the motion of the vector $\mathbf{L}$ is the plot of $M_{\perp}(\psi)$ shown in Fig. 7 for $H = 50$ kOe with change of orientation of the magnetic field in the (001) plane, obtained by reducing the curves of Fig. 3 (ψ is the angle between the field and the [010] axis). It is seen from Fig. 7 that the $M_{\perp}(\psi)$ dependence is well described by the expression $M_{\perp}(\psi) + A\sin 4\psi$. The quantity $M_{\perp}(\psi)$ has a maximum at $\psi = 22—23°$.

The existence of $M_{\perp}(H)$ at various angles in weak magnetic field is due to the onset of the magnetic moment $\sigma_{D\perp}$ when the antiferromagnetic vector is rotated

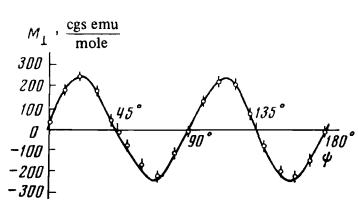

FIG. 7. Dependence of $M_{\perp}(H)$ of CoF_2 at $H = 50$ kOe on the orientation of H in the (001) plane.

in the (001) plane. Minimizing the thermodynamic potential (1) at arbitrary orientation of **H** in the (001) plane, and taking into account in (1), for the sake of simplicity, besides the invariants of the exchange interaction and the Dzyaloshinskiĭ interaction, only the anisotropy fields $H_{AE}^2 = aB$ and $H_{AE}^2 = gB$, we can obtain expressions for $M_\perp(H)$ and for the field dependences of the rotation angles $\varphi(H)$ and $\theta(H)$ of the antiferromagnetic vector **L**. In this case

$$M_\perp(H) = (e/B)(\gamma_y \cos\psi - \gamma_x \sin\psi)$$
$$= \sigma_{D\perp} \sin\theta (\sin\varphi\cos\psi - \cos\varphi\sin\psi); \quad (9)$$
$$\partial\Phi/\partial\theta = (H_{AE}^2 - H_{D\perp}^2)\sin\theta - H_{D\perp}(H_x\sin\varphi + H_y\cos\varphi),$$
$$\partial\Phi/\partial\varphi = [-(H_x\cos\varphi - H_y\sin\varphi)H_{D\perp} + H_{AE}^{*2}\sin^3\theta\sin 4\varphi]\sin\theta = 0. \quad (10)$$

It is seen from these equations that if no account is taken in (1) of the anisotropy field in the (001) or at very small rotation angles of **L**, then the angle ψ between the direction of **H** and the [010] axis is equal to the angle φ between the projection of the vector **L** on the (001) plane and the [100] axis: $H_X/H_Y = \gamma_Y/\gamma_X$, $\varphi = \psi$; in this case $M_\perp(H) = 0$. (This case was considered in[17] for CoF_2 in weak fields H, and in[7] for NiF_2 near the transition point T_N.)

If the anisotropy field in the (001) plane is taken into account in (1) in simplified form, then a projection $M_\perp(H)$ perpendicular to the field H is obtained, and the expression for it is

$$M_\perp(H) = \sigma_{D\perp}\left(\frac{H}{H_c^*}\right)^4 \frac{H_{AE}^{*2}}{H_{D\perp}H}(\cos\varphi\cos\psi + \sin\varphi\sin\psi)\sin 4\varphi. \quad (11)$$

In the considered region of magnetic fields, $H \ll H_C$, the value of the angle φ is close to the value of the angle ψ, and expression (11) is confirmed by the experimental data of Fig. 7, where $M_\perp(\psi)$ is represented in the form $M_\perp(\psi) = A \sin 4\psi$. It must be noted, however, that vanishing of $M_\perp(H)$ at $\mathbf{H} \parallel [110]$ is possible also because of the presence of two equivalent (relative to the magnetic field) domains with transverse weak ferromagnetism $\sigma_{D\perp}$[7]; however, the fact that the relation $M_\perp(H) \sim \sin 4\psi$ is satisfied confirms qualitatively the assumption that at $\mathbf{H} \parallel [110]$ the rotation of the antiferromagnetic vector **L** is in the $(1\bar{1}0)$ plane. The results showing that in weak fields at $\mathbf{H} \parallel [110]$ the antiferromagnetic vector **L** rotates in the (110) plane were obtained in a number of studies.[17,18]

By minimizing the thermodynamic potential (1) at $\mathbf{H} \parallel [110]$ we can find that when **L** is rotated in the $(1\bar{1}0)$ plane there is produced along the tetragonal axis [001] a magnetic moment

$$M_\perp^z(H) = -[\sigma_{D\perp} - \sigma_{D\parallel}]\sin^2\theta\cos\theta$$
$$-\chi_\perp(1 - \chi_\parallel/\chi_\perp)H\sin\theta\cos\theta. \quad (12)$$

It is seen from (8) and (12) that when the antiferromagnetic vector **L** is rotated in the $(\bar{1}10)$ plane towards the direction of the applied magnetic field $\mathbf{H} \parallel [110]$, there is produced along this field an additional moment

$$\sigma_D = \sigma_{D\perp}\sin\theta - (\sigma_{D\perp} - \sigma_{D\parallel})\sin^3\theta.$$

Perpendicular to the applied magnetic field, along the tetragonal axis [001], there is produced a magnetic moment

$$\sigma_D = -(\sigma_{D\perp} - \sigma_{D\parallel})\sin^2\theta\cos\theta.$$

The appearance of these magnetic moments corresponds to the fact that when the antiferromagnetic vector **L** is rotated in the $(\bar{1}10)$ plane there is produced perpendicular to the vector **L** a transverse weak ferromagnetism

$$\sigma_{D\perp}^* = \sigma_{D\perp}\sin\theta\cos\theta,$$

and in this case there is produced, parallel to the antiferromagnetic vector **L**, a longitudinal weak ferromagnetism

$$\sigma_{D\parallel}^* = \sigma_{D\parallel}\sin^2\theta.$$

Let us compare these conclusions with the experimental results shown in Figs. 4 and 5. It is seen from Fig. 4 that in a magnetic field $\mathbf{H} \parallel [010]$ the moment $M_\perp^Z(H)$ is small at all values of H. The deviation of this quantity from zero is due to the inaccurate orientation of the magnetic field relative to the (001) plane. The contribution made to $M_\perp^Z(H)$ by the inaccurate orientation of the magnetic field H relative to the (001) plane can be taken into account in the same manner as in[19], by representing $M_\perp^Z(H)$ at $\mathbf{H} \parallel [010]$ in the form $M_\perp^Z(H) = kM_\parallel(H)$, where $M_\parallel(H)$ is the magnetic moment in the (001) plane and depends linearly on H (see formula (6)). In a field H = 10 kOe, the $M_\perp^Z(H)$ contribution corresponding to formula (12) can be neglected, since it depends quadratically on the field. The obtained experimental relation $M_\perp^Z(\psi) = A \sin\psi$ at H = 10 kOe (see Fig. 5a) confirms the assumption made. From the value of A we can determine $k = \tan\alpha$, where α is the angle between the direction of the field and the (001) plane; experiments yield α on the order of 3°. It is seen from Fig. 5 that this angle lies in the (100) plane.[3)]

The obtained value of k was used to introduce a correction to the experimental $M_\perp^Z(\psi)$ curve at H = 50 kOe. The obtained curve is shown dashed in Fig. 5b. It is seen from Fig. 5 that $M_\perp^Z(H) = 0$ when H is directed along [100] or [010], and reaches a maximum $M_\perp^{Z0} = B = 360 \pm 30$ cgs emu/mole at $\mathbf{H} \parallel [110]$.

At H = 50 kOe (see Fig. 2) only a small difference is observed between the values of $M_\parallel$ at $\mathbf{H} \parallel [010]$ and $\mathbf{H} \parallel [110]$, showing that in this field the antiferromagnetic vector still does not go out of the (110) plane (it will be shown below that such a rotation begins in fields $H \sim 80$ kOe).

With the aid of the obtained value of $M_\perp^{Z0}(H = 50$ kOe), taking into account expression (12) for $M_\perp^Z(H)$, we can determine the value of the longitudinal weak ferromagnetism $\sigma_{D\parallel}$. The angle θ of rotation of the antiferromagnetic vector away from the tetragonal axis [001] can be determined from the formula $\sin\theta = H/H_c^*$. The angle θ determined in this manner for 50 kOe is equal to 19° ± 3°. When the values of $\chi_\perp$ and $\chi_\parallel$ listed in the table are used, the second term in (12) is equal to

$$\chi_\perp(1 - \chi_\parallel/\chi_\perp)H\sin\theta\cos\theta = 220 \pm 20 \text{ cgs emu/mole}.$$

The value of the first term is then

$$(\sigma_{D\perp} - \sigma_{D\parallel})\sin^2\theta\cos\theta = 140 \pm 20 \text{ cgs emu/mole}.$$

Using the value of $\sigma_{D\perp}$ from the table we can determine the longitudinal weak ferromagnetism: $\sigma_{D\parallel} = 3700 \pm 400$ cgs emu/mole.

The fact that the function $M_\perp^Z(\psi)$ in Fig. 5 takes at H = 50 kOe the form $M_\perp^Z(\psi) = B \sin 2\psi \operatorname{sgn}\sin\psi$ is explained by the reversal of the magnetization of the single crystal when the latter is rotated. If in the course of the variation of the orientation of the magnetic field **H** in the (001) plane the field were to be applied strictly in this plane, then the single crystal would break up at $\mathbf{H} \parallel [110]$ into domains that are equivalent relative to the applied magnetic field, with magnetic moments

$$M_\perp^z = (\sigma_{D\perp} - \sigma_{D\parallel}) \sin^2\theta \cos\theta - \chi_\perp (1 - \chi_\parallel/\chi_\perp) H \sin\theta \cos\theta,$$

oppositely directed along the tetragonal axis, with $M_\perp^z(H) = 0$ on the average, However, the presence of an angle $\alpha \sim 3°$ between the direction of the applied magnetic field and the (001) plane results in a component of the magnetic field H along the tetragonal axis h, which varies like $h = h_0 \sin\psi$ when the single crystal is rotated from $\psi = 0$ to $\psi = 360°$, and which remagnetizes the single crystal into a one-domain state. We then have on Fig. 5b $M_\perp^z = B \sin 2\psi(+1)$ at $0 < \psi < 180°$ and $M_\perp^z = B \sin 2\psi(-1)$ at $180 < \psi < 360°$.

We proceed now to a discussion of the experimental data in magnetic fields stronger than 50 kOe, at $H \parallel [110]$ (Fig. 2b). In strong magnetic fields, more differences are observed between the plots of $M_\parallel(H)$ at $H \parallel [010]$ and $H \parallel [110]$. It is seen from Fig. 2b that when the magnetic field is increased, $H > 70$ kOe, a magnetic moment $M_\perp(H)$ perpendicular to the applied magnetic field appears and has a nonlinear dependence on H. From the expressions for the $M_\parallel(H)$ and $M_\perp(H)$ dependences we can see that the appearance of $M_\perp(H)$ at this orientation of the magnetic field is possible only if with increasing magnetic field H the antiferromagnetic vector L, rotating away from the [001] axis, goes out of the $(\bar{1}00)$ plane and begins to rotate towards the (100) or (010) plane. This gives rise to a state with a transverse weak ferromagnetism $\sigma D\perp$ and a magnetic moment $M_\perp(H)$, equal to the projection of $\sigma_{D\perp}$ on the $[1\bar{1}0]$ direction, appears. As seen from Fig. 2b, such a rotation of L becomes noticeable at $H > 80$ kOe. From the expressions for $M_\parallel(H)$ and $M_\perp(H)$ and from the equations of motion of the antiferromagnetic vector L at arbitrary H it is seen that with further increase of the magnetic field H the antiferromagnetic vector should rotate perpendicular to the applied magnetic field.

Using the obtained $\chi_\perp$ and $\sigma_{D\perp}$, $\chi_\parallel$, and $\sigma_{D\parallel}$ (see the table) we can determine for CoF_2 the values of the effective fields $H_{D\perp} = 200 \pm 20$ kOe responsible for the transverse weak ferromagnetism and $H_{D\parallel} = 340 \pm 40$ kOe causing the longitudinal weak ferromagnetism, and also the auxiliary effective field[7] $H^*_{D\parallel} = 140 \pm 20$ kOe.

We consider now the results of the experiments on NiF_2 (Fig. 6). According to the preceding studies[6,7,10], at $H = 0$ and in weak magnetic fields at $H \parallel [010]$, a state is realized with an antiferromagnetic vector L lying in the (001) plane along the axis [100] or [010]. This gives rise to a transverse weak ferromagnetism $\sigma_{D\perp} \parallel [010]$ or [100]. When a magnetic field H is applied parallel to $[1\bar{1}0]$ (Fig. 6, curve 2), the antiferromagnetic vector L is rotated away from the [010] axis in such a way that the vector L becomes perpendicular to H; then $M_\parallel(H)$ approaches asymptotically the function $M_\parallel(H) = \chi_\perp H$ (Fig. 6, curve 4) corresponding to a state when the antiferromagnetic vector L is perpendicular to H. When the antiferromagnetic vector is rotated towards the $[1\bar{1}0]$ axis, the transverse weak ferromagnetism $\sigma_{D\perp}$ vanishes and a spontaneous magnetic moment perpendicular to the applied magnetic field and parallel to the antiferromagnetic vector L appears—the longitudinal weak ferromagnetism $\sigma_{D\parallel}$. For NiF_2 the antiferromagnetic vector L lies in the (001) plane, and therefore in expression (1) and in the expressions for $M_\parallel(H)$, $M_\perp(H)$, and $M_\perp^z(H)$ and in the equations for $\varphi(H)$ and $\theta(H)$ we must put $\theta = 90°$ and $\sin\theta = 1$, $\cos\theta = 1$. We consider here only the equation for the angle $\varphi(H)$ of rotation of the antiferromagnetic vector L in the (001) plane.[7,10]

Substituting the known data[7,10] for $\chi_\perp$, $\sigma_{D\perp}$, $\chi_\parallel$, and $\sigma_{D\perp}$ in the equation for $\varphi(H)$ and in the expressions for $M_\parallel(H)$ and $M_\perp(H)$, and solving numerically the equation for $\varphi(H)$ with a computer, we can obtain the dependence of the angle $\varphi(H)$ of rotation of the antiferromagnetic vector L on the applied magnetic field. Substituting these values of the angle $\varphi(H)$ in the expressions for $M_\parallel(H)$ and $M_\perp(H)$, we can compare the results of such a calculation with experiment (Fig. 6).

The qualitative interpretation of the experimental data shown in Fig. 6, the solution of the equation for $\varphi(H)$, and the comparison with experiment are carried out in analogy with the earlier procedures[7,10][4)] A numerical solution of the equation for the angle $\varphi(H)$ of rotation of the antiferromagnetic vector L shows that in magnetic fields $H \sim 140$ kOe the angle of rotation of L is $\sim 30°$. The contribution made to the magnetic moment $M_\perp(H)$ by the longitudinal weak ferromagnetism amounts to 30% of the obtained value of $M_\perp(H)$. The point A on Fig. 6 at $H = 140$ kOe shows the value of $M_\perp(H)$ that would be obtained if the antiferromagnetic vector were rotated through $\sim 30°$ in the absence of longitudinal weak ferromagnetism.

Knowing the values of $\chi_\perp$, $\sigma_{D\perp}$, $\chi_\parallel$, and $\sigma_{D\parallel}$ we can determine for NiF_2 the values of the effective fields responsible for the appearance of the transverse weak ferromagnetism ($H_{D\perp} = 27.2 \pm 1$ kOe) and the longitudinal weak ferromagnetism ($H_{D\parallel} = 52 \pm 2$ kOe), as well as the values of the auxiliary magnetic field $H^*_{D\parallel} = 11.2 \pm 0.2$ kOe and the exchange field $H_E = 1100 \pm 100$ kOe.

Thus, our results show that in CoF_2, upon application of a magnetic field $H \parallel [110]$ in magnetic fields up to 40—50 kOe the vector L is rotated in the $(\bar{1}10)$ plane from the tetragonal axis towards the magnetic field H. The rotation of L is accompanied by the appearance of transverse weak ferromagnetism $\sigma_{D\parallel} \sin\theta \cos\theta$ perpendicular to the rotating antiferromagnetic vector L, and a longitudinal ferromagnetic moment $\sigma_{D\parallel} \sin^2\theta$ along the rotating antiferromagnetic vector L. With increasing magnetic field $H \parallel [110]$, the antiferromagnetic vector L, rotating away from the [001] axis, goes out of the $(1\bar{1}0)$ plane. The numerical values of $\chi_\perp$, $\sigma_{D\perp}$, $\chi_\parallel$, and $\sigma_{D\perp}$ for CoF_2 are given in the table.

In NiF_2, in accord with the earlier work,[7,8] when a magnetic field $H \parallel [110]$ is applied, the antiferromagnetic vector rotates in the (001) plane towards a direction perpendicular to the applied magnetic field H, i.e., towards the [110] axis; the state with transverse ferromagnetism $\sigma_{D\perp}$ vanishes, and a state with a longitudinal weak ferromagnetism $\sigma_{D\parallel}$ appears. The numerical values of $\chi_\perp$, $\sigma_{D\perp}$, $\chi_\parallel$, and $\sigma_{D\parallel}$ for NiF_2 are given in the table.

The authors are sincerely grateful to P. L. Kapitza for constant interest in the work, to A. S. Borovik-Romanov and N. M. Kreĭnes for directing the work and for a discussion of the results, I. E. Dzyaloshinskiĭ for an evaluation of the results, and N. E. Alekseevskiĭ for interest.

[1)]International Laboratory for Strong Magnetic Fields and Low Temperatures, Wroclaw, Poland.

[2)]The authors thank S. V. Petrov for kindly supplying the CoF_2 and NiF_2 single crystals.

[3)]This angle was chosen after repeated experiments.

[4)]There is a misprint in [4,7]: the value of the g-factor in the calculation of the fields of the anisotropy energy in the (001) plane of the crystal from the antiferromagnetic-resonance data was g = 2.3.

[1]I. E. Dzyaloshinskiĭ, Zh. Eksp. Teor. Fiz. **33**, 1454 (1957) [Sov. Phys.-JETP **6**, 1120 (1958)].

[2]A. S. Borovik-Romanov, in: Itogi nauki (Science Progress) ed. Ya. G. Dorfman, Izd. Akad. Nauk SSSR **4**, 1962, p. 7.

[3]W. Stout and E. Katalano, Phys. Rev. **92**, 1575 (1953).

[4]P. L. Richard, J. Appl. Phys. **35**, 850 (1964).

[5]A. S. Borovik-Romanov, Zh. Eksp. Teor. Fiz. **38**, 1088 (1960) [Sov. Phys.-JETP **11**, 786 (1960)].

[6]L. M. Matarrese and J. W. Stout, Phys. Rev. **94**, 1792 (1954).

[7]A. S. Borovik-Romanov, A. N. Bazhan, and N. M. Kreĭnes, Zh. Eksp. Teor. Fiz. **64**, 1367 (1973) [Sov. Phys-JETP **37**, 695 (1973)].

[8]A. H. Cook, K. A. Gehring, and R. Lazenby, Proc. Phys. Soc. **85**, 967 (1965).

[9]R. J. Joenk and R. M. Bozorth, Proc. of the Internat. Conf. on Magnetism, published by the Inst. of Physics and the Physical Society, Nottingham, 1964, p. 493.

[10]A. N. Bazhan, Zh. Eksp. Teor. Fiz. **65**, 2479 (1973) [Sov. Phys.-JETP **38**, 1238 (1974)].

[11]V. I. Ozhogin, Candidate's dissertation, Kurchatov Inst. of Atomic Energy, 1965.

[12]S. Foner, Proc. of the Internat. Conf. on Magnetism, published by the Inst. of Physics and the Physical Society, Nottingham, 1964, p. 438.

[13]Yu. M. Gufan, K. N. Kocharyan, A. S. Prokhorov, and E. G. Pudashevskiĭ, Zh. Eksp. Teor. Fiz. **66**, 1155 (1974) [Sov. Phys.-JETP **39**, 565 (1974)].

[14]A. N. Bazhan, A. S. Borovik-Romanov, and N. M. Kreĭnes, Prib. Tekh. Eksp. No. 1, 213 (1973).

[15]N. M. Kreĭnes, Zh. Eksp. Teor. Fiz. **40**, 762 (1961) [Sov. Phys.-JETP **13**, 534 (1961)].

[16]R. Z. Levitin, Pis'ma Zh. Eksp. Teor. Fiz. **9**, 318 (1968) [JETP Lett. **9**, 187 (1968)].

[17]A. S. Prokhorov and E. G. Pudashevskiĭ, Pis'ma Zh. Eksp. Teor. Fiz. **10**, 175 (1969) [JETP Lett. **10**, 110 (1969)].

[18]V. I. Ozhorin, Doctoral dissertation, Kurchatov Institute of Atomic Energy, 1974.

[19]A. N. Bazhan and N. M. Kreĭnes, Pis'ma Zh. Eksp. Teor. Fiz. **15**, 537 (1972) [JETP Lett. **15**, 380 (1972)].

Translated by J. G. Adashko
190